Engineering Plasminogen Activator Inhibitor 1 Mutants with Increased Functional Stability†

D. A. Lawrence,*,‡ S. T. Olson,§ S. Palaniappan,‖ and D. Ginsburg‡,‖,⊥

Departments of Internal Medicine and Human Genetics and Howard Hughes Medical Institute, 4520 MSRB I, University of Michigan, Ann Arbor, Michigan 48109-0650, and Henry Ford Hospital, 2799 West Grand Boulevard, Detroit, Michigan 48202-2689.

Received November 1, 1993; Revised Manuscript Received January 25, 1994®

ABSTRACT: Plasminogen activator inhibitor 1 (PAI-1), a member of the serine protease inhibitor (Serpin) superfamily, is the primary inhibitor of the plasminogen activators tPA and uPA. PAI-1 is produced in an active form but converts to an inactive or latent form with a half-life of approximately 1 h at pH 7.5, 37 °C. This study describes the construction, expression, and characterization of PAI-1 mutants with increased functional stability. Three mutations that disrupt an ion pair, present in latent PAI-1, between Arg-30 and Glu-350 (P4′), were introduced into recombinant PAI-1. All three mutant proteins maintained normal functional activity against both uPA and tPA. However, the half-life of each purified PAI-1 mutant was extended compared to the 1.1 h observed for wild-type PAI-1 (wtPAI-1) (1.2 h for Glu-350 → Arg, 2.0 h for Glu-350 → Pro, and 2.1 h for the Arg-30 → Glu mutation). An additional PAI-1 variant containing a second mutation designed to potentially reconstitute the ion pair (Arg-30 → Glu, Glu-350 → Arg) failed to restore the wild-type half-life. Circular dichroism spectra analysis indicated that the active and latent forms of wtPAI-1 and all four mutants contained similar secondary structural elements. Thermal stability determinations showed that latent wtPAI-1 was much more structurally stable than the active conformation. However, the latent form for all four mutants was significantly less stable than the corresponding wtPAI-1 conformer. This is the first report of PAI-1 mutants which have been specifically engineered to produce enhanced functional stability.

Plasminogen activators (PAs)[1] are specific serine proteases that activate the proenzyme plasminogen to the broad-specificity enzyme plasmin by cleavage of a single Arg–Val peptide bond (Saksela, 1985). Two plasminogen activators are known to occur in mammals: tissue-type PA (tPA) and urokinase-type PA (uPA) (Saksela & Rifkin, 1988). These enzymes are thought to critically influence many biological processes, including vascular fibrinolysis (Bachmann, 1987), ovulation (Ohlsson et al., 1991), inflammation (Pöllänen et al., 1991), tumor metastasis (Dano et al., 1985), angiogenesis (Moscatelli & Rifkin, 1988), and tissue remodeling (Saksela & Rifkin, 1988). Plasminogen activator inhibitor 1 (PAI-1) is considered to be one of the principal regulators of the PA system (Lawrence & Ginsburg, 1994). It is a single-chain glycoprotein with a molecular mass of 50 kDa (van Mourik et al., 1984) and is the most efficient inhibitor known of tPA and uPA (Lawrence et al., 1989). PAI-1 belongs to the serine protease inhibitor superfamily (Serpins) (Carrell & Travis, 1985). This gene family includes many of the protease inhibitors found in blood, as well as other proteins with unrelated or unknown functions (Huber & Carrell, 1989). PAI-1 is found in plasma at very low concentrations, is present in platelets and many other tissues, and is produced by many cells in culture (Sawdey & Loskutoff, 1991; Krishnamurti & Alving, 1992). In plasma, PAI-1 is present as a complex with vitronectin or S protein (Declerck et al., 1988). PAI-1 is also associated with vitronectin in the extracellular matrix in culture and may be involved in maintaining the integrity of the cell substratum *in vivo* (Mimuro & Loskutoff, 1989).

PAI-1 exists in at least two conformations: an active form that is produced by cells and secreted into the culture medium and an inactive or latent form that accumulates in the media over time (Hekman & Loskutoff, 1985; Levin & Santell, 1987). The active form spontaneously converts to the latent form with a half-life of about 1 h at 37 °C at neutral or slightly alkaline pH (Levin & Santell, 1987; Hekman & Loskutoff, 1988; Lawrence et al., 1989; Lindahl et al., 1989). The latent form can be converted into the active form by treatment with denaturants, negatively charged phosphlipids, or vitronectin, though the latter reaction is very slow (Hekman & Loskutoff, 1985; Lambers et al., 1987; Wun et al., 1989). In one report, analysis of latent PAI-1 infused into rabbits suggests that reactivation may also occur *in vivo*, though the exact mechanism remains unknown (Vaughan et al., 1990). The latent form appears to be more energetically favorable, since the conversion to latent is spontaneous, while the conversion from latent to active requires more extreme treatment (Hekman & Loskutoff, 1985; Katagiri et al., 1988). The three-dimensional structure of latent PAI-1 was recently reported. In this structure, the entire amino-terminal side of the reactive center loop is inserted as the central strand into β-sheet A (Mottonen et al., 1992). While the structure of active PAI-1 is unknown, it has been proposed that the reactive

† This work was supported in part by National Institutes of Health Grants HL 08572 (D.A.L.), HL 39137 (D.G.), and HL 39888 (S.T.O.).

* To whom correspondence should be addressed at Room 4520, MSRB I, University of Michigan, Ann Arbor, MI 48109-0650.

‡ Department of Internal Medicine, University of Michigan.

§ Henry Ford Hospital.

‖ Howard Hughes Medical Institute, University of Michigan.

⊥ Department of Human Genetics, University of Michigan.

® Abstract published in *Advance ACS Abstracts,* March 1, 1994.

[1] Abbreviations: PAs, plasminogen activators; uPA, urokinase plasminogen activator; tPA, tissue-type plasminogen activator; PAI-1, plasminogen activator inhibitor 1; wtPAI-1, wild-type plasminogen activator inhibitor 1; SDS–PAGE, sodium dodecyl sulfate–polyacrylamide gel electrophoresis; Tris, tris(hydroxymethyl)aminomethane; Tween 80, polyoxyethylene sorbitan monooleate; CD, circular dichroism; PBS, phosphate-buffered saline.

0006-2960/94/0433-3643$04.50/0

center loop in active PAI-1 is exposed on the surface, similar to the structure of the noninhibitory Serpin ovalbumin (Stein et al., 1990). In latent PAI-1, a salt bridge is present between Arg-30 and the P4′ residue of the reactive center loop (Glu-350), and comparison of this structure with that of ovalbumin suggests that the salt bridge would not exist in active PAI-1. We propose that this ionic interaction favors the latent structure and thereby could affect the conversion of active to latent PAI-1. To examine this hypothesis, we produced a set of site-directed mutants of PAI-1 which disrupt this salt bridge. All of these mutants demonstrate a decreased structural stability for the latent form and an increased functional half-life for active PAI-1.

EXPERIMENTAL PROCEDURES

Site-Directed Mutagenesis of PAI-1. Mutagenesis was performed using the *Altered Sites* mutagenesis kit following the manufacturer's instructions (Promega). Briefly, the PAI-1 cDNA, along with T7 promoter and terminator regulatory sequences, was isolated as an *Xba*I–*Eco*RV fragment from the PAI-1 expression plasmid pET_{3a}PAI-1 (Sherman et al., 1992). This fragment was ligated to *Pst*I/*Xba*I-cut pSELECT-1 (Promega) that had been blunt-ended at the *Pst*I site, creating phagemid pSELPAI-1. This construct was then transformed into *Escherichia coli* strain JM109, and single-stranded DNA was produced by infection with the helper phage R408 (Promega). PAI-1 mutant constructs were produced using the following oligonucleotides: Arg-30 → Glu, oligonucleotide A, GCCTCCAAGGACGAGAACGTG-GTTTTC; Glu-350 → Arg, oligonucleotide B, CGCATG-GCCCCCAGGGAGATCATCATG; and Glu-350 → Pro, oligonucleotide C, CGCATGGCCCCCCCGGAGATCAT-CATG. For construction of the double-mutant Arg-30 → Glu, Glu-350 → Arg, both oligonucleotides A and B were used simultaneously. The integrity of all mutant clones selected for protein expression was confirmed by DNA sequence analysis of the entire coding region.

Expression, Purification, and Characterization of PAI-1. The inclusion of T7 promoter and terminator sequences in the pSELPAI-1 constructs permitted efficient PAI-1 expression directly from this vector using an *E. coli* strain producing T7 polymerase (Studier et al., 1990). Briefly, *E. coli* strain BL21 (DE3) transformed with the pSELPAI-1 mutants was grown to an OD_{650} of 0.5, PAI-1 production was induced by the addition of 1 mM isopropyl β-D-thiogalactoside, and growth was continued at 37 °C for 2 h. Cells were harvested, and PAI-1 was purified as described (Lawrence et al., 1989; Sherman et al., 1992). Protein yields were approximately 1–5 mg/L of cell culture. Purity was assessed by SDS–PAGE and staining by Coomassie blue. Inhibitory activity against both uPA (American Diagnostica) and tPA (Activase, Genentech) was measured in a single-step chromogenic assay as described (Lawrence et al., 1989) and compared to wtPAI-1 purified from *E. coli* carrying the expression plasmid pET_{3a}-PAI-1 (Sherman et al., 1992). All the mutant proteins had specific activities similar to wild-type PAI-1, demonstrating approximately 50% of the calculated maximum theoretical specific activity (Lawrence et al., 1989).

Determination of the Functional Half-Lives ($T_{1/2}$) at 37 °C. PAI-1 was diluted to 10 μg/mL in assay buffer (150 mM NaCl, 50 mM Tris, pH 7.5, 100 μg/mL bovine serum albumin, and 0.01% Tween 80), and the uPA inhibitory activity was determined. This time point was designated as T_0, and the relative amount of inhibitory activity was considered to be 100%. The samples were next incubated at 37 °C, and at the times indicated, aliquots were removed and reassayed for remaining uPA inhibitory activity. The percent remaining uPA inhibitory activity relative to the amount at T_0 was then calculated.

Binding of Active PAI-1 to Vitronectin. Vitronectin purified under nondenaturing conditions (Naski et al., 1993) was a generous gift from Dr. D. Mosher. Binding of active PAI-1 to vitronectin was determined in a functional binding assay, on vitronectin-coated (1 μg/mL) Immulon 2 (Dynatech) microtiter plates as described (Lawrence et al., 1990). The concentration of active PAI-1 added was determined in solution by titration with uPA. The concentration of active PAI-1 bound was calculated from the percent of uPA inhibition, on the basis of the known molecular masses of PAI-1 (43 kDa) and uPA (52 kDa) and the specific activity of uPA (100 IU/μg), and assuming a 1:1 stoichiometry between PAI-1 and uPA (Lawrence et al., 1989).

Circular Dichroism (CD) Spectra Analysis and Thermal Denaturation Studies. Samples were diluted to approximately 200 μg/mL, dialyzed into 150 mM NaCl/50 mM Tris, pH 7.5, and then incubated for 24 h at 37 °C, followed by extensive dialysis against 50 mM sodium phosphate buffer, pH 6.6. Active PAI-1 samples, at similar concentrations, were also dialyzed into sodium phosphate buffer. To correct for loss of protein during treatment and dialysis, the protein concentration and functional activity of all samples were again determined after dialysis. Protein concentrations were determined by measuring OD_{280} and assuming an absorbance of 1.0 for 1 mg/mL PAI-1 ($\epsilon_{1\%}$ = 10). For CD spectra analysis, the samples were diluted to 40 μg/mL in 50 mM sodium phosphate buffer, pH 6.6, and added to a 1-cm path-length quartz cuvette. Spectra were determined over a wavelength range of 190–260 nm at 25 °C in a JASCO J-600 spectropolarimeter with a bandwith of 1 nm and a 0.2-nm step resolution. Thermal denaturation analysis was performed in the same spectropolarimeter over the temperature range 35–75 °C at a constant wavelength of 222 nm. The step resolution was 0.1 °C, and the temperature slope was 50 °C/h. Similar melting transitions were generated when the temperature slope was increased by a factor of 2 (data not shown), consistent with equilibrium being maintained throughout the transition.

CD melting curves were analyzed by the van't Hoff equation (Edsall & Gutfreund, 1984):

$$\Delta G^\circ = -RT \ln\left(\frac{\theta_{obs} - \theta_N}{\theta_D - \theta_{obs}}\right) = \Delta H_m\left(1 - \frac{T}{T_m}\right) \quad (1)$$

where R is the gas constant, T the temperature in degrees kelvin, θ_{obs} the observed ellipticity at temperature T, θ_N and θ_D the ellipticities of native and denatured states, respectively, at temperature T, ΔH_m the van't Hoff enthalpy change for thermal unfolding, and T_m the melting temperature at the midpoint of the melting transition. θ_N and θ_D in this equation are assumed to vary linearly with temperature over the range studied according to

$$\theta_N = \theta_N^\circ + m_N T, \theta_D = \theta_D^\circ + m_D T \quad (2)$$

where θ_N°, θ_D° and m_N, m_D are the intercepts and slopes, respectively, of this linear dependence. Solving the above equation for θ_{obs} as a function of T gives

$$\theta_{obs} = \frac{\theta_N + \theta_D \exp[(-\Delta H_m/R)(1/T - 1/T_m)]}{1 + \exp[(-\Delta H_m/R)(1/T - 1/T_m)]} \quad (3)$$

Melting curves were determined by computer-fitting 400 data points collected over the temperature interval between 35 and 75 °C at 0.1 °C steps by this equation using standard nonlinear

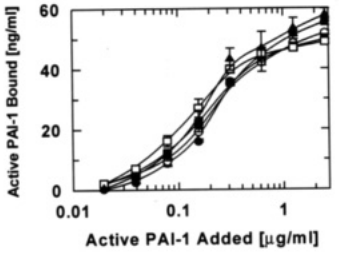

FIGURE 1: Binding of active PAI-1 to vitronectin. Plot of active PAI-1 bound vs active PAI-1 added to vitronectin-coated microtiter plates. PAI-1 concentrations were calculated as described under Experimental Procedures, and bound PAI-1 was determined by measuring the uPA inhibitory activity bound to the plate. Points represent the average of four determinations except for wtPAI-1 which is the average of two experiments. The curves are a best fit of the data by the GraFit program (Erithacus Software). wtPAI-1 (●); Arg-30 → Glu (▲); Glu-350 → Arg (□); Glu-350 → Pro (○); Arg-30 → Glu, Glu-350 → Arg (■). Standard errors (SEM) for each point are shown except where the values are smaller than the symbol.

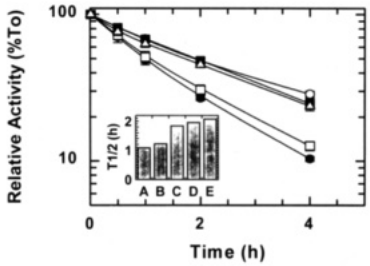

FIGURE 2: log-linear plot of the percent remaining PAI-1 inhibitory activity toward uPA vs time. The plots were drawn with the GraFit Program (Erithacus Software), and each point represents the average of three to four separate experiments (except for the 1 h time point of the Glu-350 → Pro mutant which is the average of two experiments). Standard errors (SEM) for each point are indicated, except where the values are smaller than the symbol shown. wtPAI-1 (●); Arg-30 → Glu (○); Glu-350 → Arg (□); Glu-350 → Pro (■); Arg-30 → Glu, Glu-350 → Arg (△). The inset shows the half-lives calculated from a linear regression fit of these data by the GraFit Program (Erithacus Software). wtPAI-1 (A); Glu-350 → Arg (B); Arg-30 → Glu, Glu-350 → Arg (C); Glu-350 → Pro (D); Arg-30 → Glu (E).

regression methods to generate values of ΔH_m and T_m for wild-type and mutant PAI-1s in both active and latent forms (Duggleby, 1984). These parameters were used to calculate the stabilities of mutants relative to wtPAI-1, $\Delta\Delta G°$, at the melting temperature for wtPAI-1, i.e., 50.2 °C for the active form and 67.5 °C for the latent form (Table 1), from the equation (Becktel & Schellman, 1987):

$$\Delta\Delta G° = \Delta G°_{\text{mutant}} - \Delta G°_{\text{wild-type}} = \Delta H_{\text{m,mutant}}(1 - T_{\text{m,wild-type}}/T_{\text{m,mutant}}) \quad (4)$$

RESULTS

Expression, Isolation, and Characterization of PAI-1s. Site-directed mutagenesis was performed to examine the possibility that the ion pair between Arg-30 and Glu-350 contributes to the stability of the latent structure. A novel phagemid vector for efficient mutagenesis and protein expression was designed. This construct, pSELPAI-1, eliminates the need to isolate and subclone each new mutant into an expression plasmid. Using this system, site-directed mutagenesis was generally achieved with greater than 50% efficiency. In addition, sequence analysis of greater than 10 kb, from eight independent clones, has identified no other mutations, indicating a very low rate of secondary mutations (less than 0.01%). The mutant proteins were purified as described (Lawrence et al., 1989, 1990), resulting in final yields of 1–5 mg/L of bacterial culture. This was significantly lower than with the parental pET_{3a}PAI-1 wtPAI-1 construct (up to 20 mg/L) (Sherman et al., 1992). However, the chromatographic profiles of each mutant, from every step of the purification, were similar to those with wtPAI-1. Of note, identical elution profiles were observed from heparin–Sepharose, suggesting that none of the mutations significantly affect heparin binding. The interaction of each mutant with vitronectin was also analyzed, and these results are shown in Figure 1. All four PAI-1 mutants were observed to bind vitronectin with approximately the same affinity as wtPAI-1. Finally, the mutant PAI-1s all have inhibitory activity toward uPA and tPA similar to wtPAI-1 (data not shown).

Functional Stability of Mutant and wtPAI-1. The functional stability of wtPAI-1 and all four mutants was examined by measuring the uPA inhibitory activity remaining in each sample following different times of incubation at 37 °C. The results of this analysis are shown in Figure 2. An approximately linear decay is seen for each inhibitor in the log-linear plot, consistent with a first-order reaction for the conversion of active to latent PAI-1 and similar to previous reports with wtPAI-1 (Lawrence et al., 1989, 1990; Declerck et al., 1988). The inset in Figure 2 shows the relative half-lives for wtPAI-1 and each mutant calculated from these data. This analysis reveals an approximate doubling of the $T_{1/2}$ for the Arg-30 → Glu mutation and the Glu-350 → Pro mutation. In contrast, the Glu-350 → Arg mutation only slightly prolongs the $T_{1/2}$ from 1.1 to 1.2 h. Finally, the double mutant Arg-30 → Glu, Glu-350 → Arg is also approximately twice as stable as wtPAI-1.

CD Analysis of Active and Latent Forms of PAI-1. CD spectra were obtained for the active and latent forms of wtPAI-1 and each mutant. Panel A of Figure 3 shows the spectra of the active forms and panel B the latent forms for wtPAI-1 and each mutant. All four mutant PAI-1s are seen to have CD spectra similar to wtPAI-1 in both the active and latent conformations, suggesting that these mutations do not significantly alter PAI-1 secondary structures. Furthermore, both active (panel A) and latent (panel B) forms of PAI-1 have similar secondary structures, in agreement with previous reports (Strandberg et al., 1991). The significance of the apparent slight differences in the spectra between 190 and 205 nm is unclear.

Comparison of the Melting Points of Active and Latent PAI-1s. The T_ms of both the active and latent conformations of wtPAI-1 and each mutant were determined by monitoring the changes in negative ellipticity at 222 nm over a temperature range of 35–75 °C. Figure 4 shows thermal denaturation curves of active and latent wtPAI-1 along with a best fit of these data. While both forms of PAI-1 appear to unfold to the same extent, as judged by similar limiting values of ellipticity, the unfolding transition of active PAI-1 occurred at a much lower temperature than that of latent (approximately 50 °C compared to 67.5 °C).

The hypothesis that the ion pair between Arg-30 and Glu-350 stabilizes the latent PAI-1 structure predicts that the latent forms of the PAI-1 mutants, which are unable to form this salt bridge, should show a decrease in thermal stability. The analysis of the melting behavior of the active and latent forms of each mutant compared to wtPAI-1 is shown in Figure 5. Panel A shows the fitted curves for the active form of each inhibitor and demonstrates that the melting behaviors of active Glu-350 → Arg and Glu-350 → Pro are nearly unaffected, whereas active Arg-30 → Glu and the double mutant appear to be slightly destabilized relative to wtPAI-1 (approximately 2 °C). In contrast, the latent conformers of all four PAI-1 mutants are significantly destabilized compared to wtPAI-1,

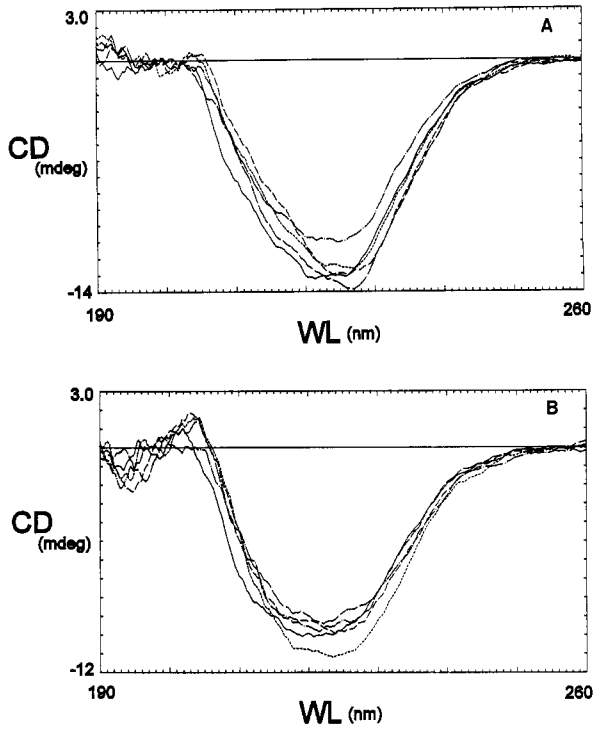

FIGURE 3: CD spectra of wtPAI-1 and each variant. Panel A shows spectra for the active PAI-1s and panel B those for latent PAI-1s. CD spectra were determined from 190 to 260 nm at protein concentrations of 40 μg/mL. Spectropolarimeter settings were as follows: bandwidth 1.0 nm, sensitivity 50 mdeg, response 1 s, step resolution 0.2 nm/min, and scan speed 200 nm/min. Each spectrum is the average of four determinations. Background buffer absorbance has been subtracted. wtPAI-1 (—); Arg-30 → Glu (···); Glu-350 → Arg (– –); Glu-350 → Pro (– · –); Arg-30 → Glu, Glu-350 → Arg (- - -).

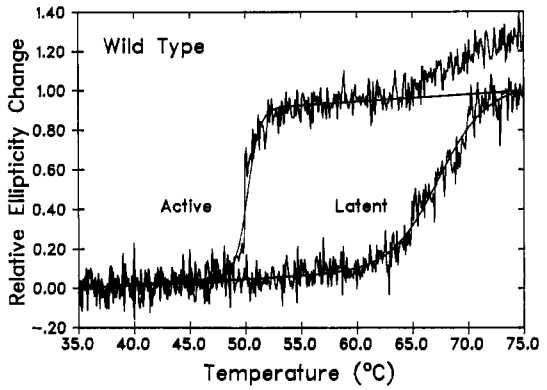

FIGURE 4: Melting curve of wtPAI-1 active and latent conformations. Relative ellipticity change at 222 nm is plotted vs temperature, over the range of 35–75 °C. The original data for both active and latent wtPAI-1s are shown along with a best-fit curve. Protein concentrations were 40 μg/mL, and spectropolarimeter settings were as follows: bandwidth 1.0 nm, sensitivity 50 mdeg, response 1 s, step resolution 0.1 °C, and temperature slope of 50 °C/h. Relative ellipticities were calculated as $(\theta_{obs} - \theta_{min})/(\theta_{max} - \theta_{min})$, where θ_{min} and θ_{max} are fitted values of ellipticity at 35 and 75 °C, respectively, and θ_{obs} is the observed ellipticity at temperature T. The melting curve for the active form was fit over the range 35–62 °C, and θ_{max} was taken as the fitted value at 62 °C due to the small latent transition evident in this curve at higher temperatures.

with the maximum decrease in T_m being about 7–8 °C for the Arg-30 → Glu mutation (panel B). These data are consistent with the hypothesis that loss of the ion pair between Arg-30 and Glu-350 results in a selective destabilization of the PAI-1 latent conformation. Furthermore, these results suggest that this loss of structural stability may, at least in part, contribute to the extended $T_{1/2}$s observed for these mutants (Figure 2).

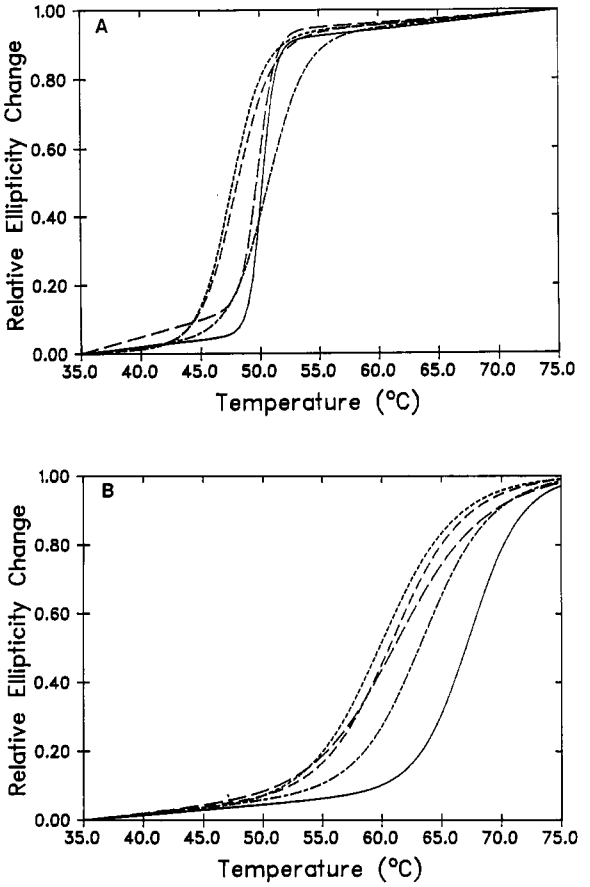

FIGURE 5: Melting curves of wtPAI-1 and PAI-1 mutants in both active and latent conformations. Panel A depicts the results for the active PAI-1s and panel B for latent PAI-1s. Each curve is a best fit of plots of the relative ellipticity change at 222 nm vs temperature over the range of 35–75 °C. Data above 62 °C were excluded from fits of the active forms when latent transitions were evident. Protein concentration and spectropolarimeter settings were as in Figure 4. wtPAI-1 (—); Arg-30 → Glu (···); Glu-350 → Arg (– –); Glu-350 → Pro (– · –); Arg-30 → Glu, Glu-350 → Arg (- - -).

Table 1[a]

	active		latent		
PAI	T_m (°C)	$\Delta\Delta G°$ (kcal/mol)	T_m (°C)	$\Delta\Delta G°$ (kcal/mol)	ΔT_m (°C)
wtPAI-1	50.2 ± 0.3	0	67.5 ± 1	0	17.3 ± 1.3
R30E	47.6 ± 0.3	−1.2 ± 0.4	60.0 ± 1	−1.7 ± 0.6	12.4 ± 1.3
E350R	49.7 ± 0.2	−0.3 ± 0.5	61.0 ± 2	−1.3 ± 0.9	11.3 ± 2.2
E350P	50.7 ± 0.8	+0.3 ± 0.5	64.0 ± 2	−0.9 ± 1.0	13.3 ± 2.8
R30E,E350R	48.0 ± 0.3	−0.9 ± 0.3	61.0 ± 1	−1.5 ± 0.7	13.0 ± 1.3

[a] Melting temperatures and $\Delta\Delta G°$ values were determined from fits of melting curves in Figure 5 to the van't Hoff equation and from eq 4, as described under Experimental Procedures. Errors in T_m and ΔH, determined from the fitting procedure, were propagated by standard statistical methods in calculations of ΔT_m and $\Delta\Delta G°$. Errors represent ±1 SE.

Thermodynamic Analysis of the Heat Denaturation of Active and Latent PAI-1s. Thermodynamic analysis of the melting behavior for each PAI-1 is summarized in Table 1. The T_ms of the active conformations are again seen to be similar to wtPAI-1, being decreased by no more than 2.6 °C. In contrast, all four mutants show significant loss of thermal stability in the latent conformation, with a maximum decrease of 7.5 °C. In addition, the difference in T_ms between the active and latent conformations (ΔT_m, Table 1) is decreased by about 5 °C for all of the mutants relative to wtPAI-1, indicating that in each case the latent conformer is significantly more destabilized than the active form by these mutations. The relative thermal stabilities of each mutant compared to

wtPAI-1 in either conformation were also determined from these data and are shown in Table 1 as $\Delta\Delta G°$. In the active conformation, both Glu-350 mutants show little change in the free energy of unfolding. However, for the two Arg-30 mutants, there is an approximately −1 kcal/mol change in $\Delta G°$, suggesting that these mutations destabilize the active conformation to some degree. Analysis of the latent conformers shows that all four mutants have differences in $\Delta G°$ ranging from −0.9 to −1.7 kcal/mol. This change is approximately that expected from the loss of a stabilizing salt bridge (Fersht, 1972).

DISCUSSION

PAI-1 is unusual among Serpins in that it is produced in an active form but readily converts to an inactive, latent form (Hekman & Loskutoff, 1985). Recently the three-dimensional protein structure of latent PAI-1 was solved, and a salt bridge was noted in this structure between residues Arg-30 and Glu-350. This ion pair has not been observed in other Serpin structures and thus appears to be unique to the PAI-1 latent conformation (Mottonen et al., 1992). We hypothesized that disruption of this ionic interaction should destabilize the latent structure, and thereby may enhance the effective functional stability of the active conformation. This report describes the construction and chracterization of PAI-1 mutants with extended functional half-lives. Analysis of the $T_{1/2}$s of the PAI-1 mutants showed that in each case the half-life was extended compared to wtPAI-1 (up to 2-fold, Figure 2). One mutant, Glu-350 → Arg, was only minimally more stable than wtPAI-1. In contrast, exchanging Glu-350 for Pro instead of Arg results in an approximate doubling of the $T_{1/2}$. In addition, the double mutant Arg-30 → Glu, Glu-350 → Arg is also nearly twice as stable as wtPAI-1. Taken together, these results suggest that mutation of either Arg-30 or Glu-350 can result in an increase in the functional half-life of active PAI-1, possibly by disrupting the salt bridge between these two residues present in the latent structure. The small change in $T_{1/2}$ observed with the Glu-350 → Arg mutation, compared to the other Glu-350 mutants, indicates that the magnitude of the effect on $T_{1/2}$ is dependent on the choice of mutant residue and suggests that additional interactions can occur that affect the active to latent transition. Interestingly, the effect of the Arg-30 → Glu mutation appears to be dominant over Glu-350 → Arg, since the half-life and thermal stability of the double mutant are similar to those of the Arg-30 → Glu single mutant alone. Finally, the failure of the double mutant to restore the wtPAI-1 half-life is probably explained by the lack of sufficient flexibility in the three-dimensional structure of PAI-1 to permit reconstitution of an ion pair in the opposite orientation, given the differences in side-chain length between Glu and Arg.

Madison and co-workers demonstrated that mutations at Arg-304 of tPA blocked the interaction of tPA with PAI-1 (Madison et al., 1989, 1990a,b) and suggested that in the tPA–PAI-1 complex this residue forms a salt bridge with Glu-350 of PAI-1. Consistent with this hypothesis, substitution of Glu-350 in PAI-1 partially restored inhibitory activity toward the mutant tPA (Madison et al., 1990b). However, the activity of this PAI-1 mutant toward wild-type tPA was indistinguishable from wtPAI-1. This latter result is consistent with our observations that substitution of Glu-350 with either Arg or Pro does not significantly affect PAI-1 inhibitory activity toward wild-type tPA. Taken together, these observations suggest that Glu-350 may be able to form alternative inter- or intramolecular ionic interactions, depending on the PAI-1 conformation, and this may represent a potential mechanism for regulating the expression of PAI-1 activity.

PAI-1 binds to the plasma glycoprotein vitronectin with high affinity, and this interaction has been shown to prolong the functional half-life of PAI-1 by approximately 2-fold (Declerck et al., 1988). Since the mutations described here result in a similar stabilization of the PAI-1 active conformation, we tested the ability of each mutant to bind vitronectin (Figure 1), and observed no significant difference compared to wtPAI-1. Though these results suggest that the mutations are unlikely to be located within the PAI-1 binding domain for vitronectin, vitronectin binding could alter PAI-1 stability by preventing the conformational change that leads to formation of the intramolecular salt bridge between Arg-30 and Glu-350. The equivalent magnitudes of stabilization observed with mutations that disrupt the salt bridge, and with vitronectin binding [Figure 2 and Declerck et al. (1988)], are consistent with this hypothesis.

To determine if the increased functional stability of the mutants correlated with a decrease in the structural stability of latent PAI-1, due to loss of the salt bridge, CD spectra analysis and thermal stability studies were performed. The results of these analyses indicated that the proteins all have similar secondary structures, suggesting that the effects of the mutations on PAI-1 structure are local (Figure 3). Consistent with this, all four mutants have similar inhibitory activity against uPA and tPA as well as normal binding to both heparin (data not shown) and vitronectin (Figure 1). Thermal denaturation analysis of wtPAI-1 indicates that latent PAI-1 is much more thermally stable than active PAI-1 (Figure 4 and Table 1). This is in agreement with earlier reports examining PAI-1 solubility as a function of temperature (Munch et al., 1991). Consistent with the hypothesis that disruption of the ion pair would decrease the stability of the latent structure, the latent forms of all four mutants demonstrated significantly lower T_ms than that of wtPAI-1 (Figure 5, panel B). Thermodynamic analysis of these data indicated a decrease in thermostability relative to that of wtPAI-1 of −1 to −2 kcal/mol. This is in the range expected for the loss of a salt bridge (Fersht, 1972). In contrast, the mutations have lesser or no effects on the stability of the active structures as demonstrated by the smaller changes in T_m and $\Delta\Delta G°$. These observations indicate that the predominant effect of the mutations is to destabilize the latent structure to an extent consistent with the loss of a stabilizing salt bridge. It should be noted that the determination of $T_{1/2}$ was performed at pH 7.5 while the thermal stability studies were carried out at pH 6.6. However, within this neutral pH range, the mutated residues (Arg and Glu) are not likely to change their state of ionization, and thus, while the absolute stabilities may show a pH dependence, the relative ordering of the thermal stabilities of wtPAI-1 and each of the mutants should not be significantly affected over this range.

For three of the four mutants, the destabilization of the latent structure produced by loss of the salt bridge correlates with an approximate doubling of the functional half-life, suggesting that this ion pair may play a role in determining the $T_{1/2}$. However, the minimal increase in the functional half-life observed with the Glu-350 → Arg mutant indicates that other factors are also influencing the $T_{1/2}$. The conversion of PAI-1 from the active to the latent state should be governed by the activation energy necessary to reach a transition-state structure intermediate between that of the active and latent structures. It is possible that a fully or partially formed salt bridge contributes to the stabilization of the transition state. If the transition state was destabilized by the mutations to the same extent as the latent structure, then the observed −1 to −2 kcal/mol decrease in stability of the latent conformer would

be expected to increase the functional half-life by about 1 order of magnitude. (A 1.4 kcal/mol increase in the activation energy would increase $T_{1/2}$ by 10-fold at 37 °C.) The maximum 2-fold increase in the functional half-life observed for the mutants corresponds to an approximate 0.4 kcal/mol increase in the activation energy at 37 °C. These observations suggest that the ion pair may make a lesser contribution to the stabilization of the transition state than it does to the latent state, due to incomplete salt bridge formation in the transition state. Alternatively, the active state may also be destabilized so as to produce an offsetting decrease in the activation energy. This possibility may be particularly relevant to the Arg-30 → Glu mutation where the active state is destabilized for both the single and the double mutant by approximately −1 kcal/mol (Table 1). The mutant side chains may also form alternative interactions in the transition state that compensate for the loss of the salt bridge. This latter possibility may explain the smaller increase in the functional half-life for the Glu-350 → Arg mutation. Thus, the loss of the salt bridge in this mutant may be compensated for by the ability of the mutant Arg side chain to form an alternative electrostatic interaction in the transition state. Such an explanation is supported by the observation that the Glu-350 → Pro mutant which is incapable of ionic interactions leads to the same 2-fold increase in $T_{1/2}$ observed with the Arg-30 → Glu mutations.

In summary, we describe the construction and characterization of novel PAI-1 mutants with increased functional half-lives relative to wtPAI-1. This is the first report of PAI-1 proteins with greater functional stability and demonstrates that the rate of conversion of active PAI-1 to the latent state can be modulated by single amino acid substitutions that do not affect other PAI-1 functions. Our data suggest that the ion pair between residues Arg-30 and Glu-350 present in the latent conformation contributes to the stability of the latent structure and that disruption of this ionic interaction may favor the active form of PAI-1 by decreasing the stability of the latent conformation and the associated intermediate transition state. The extent to which the active form is favored in each mutant appears to be influenced by the nature of the specific amino acid substituted. These observations suggest that the active state of PAI-1 may be a metastable conformation that can be favored by decreasing the stability of the end-state conformation and provide an interesting example whereby the functional stability of a protein has been increased by introducing mutations that decrease its structural stability.

ACKNOWLEDGMENT

We thank P. Andrews, R. Ogorzalek Loo, and M. Sandkvist for helpful discussions, S. Labun for assistance in preparation of the manuscript, and The University of Michigan Biomedical Research Core Facilities for use of the spectropolarimeter.

REFERENCES

Bachmann, F. (1987) in *Thrombosis Haemostasis* (Verstraete, M., Vermylen, J., Linjen, H. R., & Arnout, J., Eds.) pp 227–265, Leuven University Press, Leuven, Belgium.

Becktel, W. J., & Schellman, J. A. (1987) *Biopolymers 26*, 1859–1877.

Carrell, R., & Travis, J. (1985) *Trends Biochem. Sci.*, 20–24.

Dano, K., Andreasen, P. A., Grondahl-Hansen, J., Kristensen, P., Nielsen, L. S., & Skriver, L. (1985) *Adv. Cancer Res. 44*, 139–266.

Declerck, P. J., De Mol, M., Alessi, M. C., Baudner, S., Pâques, E.-P., Preissner, K. T., Müller-Berghaus, G., & Collen, D. (1988) *J. Biol. Chem. 263*, 15454–15461.

Duggleby, R. G. (1984) *Comput. Biol. Med. 14*, 447–455.

Edsall, J. T., & Gutfreund, H. (1984) in *Biothermodynamics: The Study of Biochemical Processes at Equilibrium*, John Wiley & Sons, New York.

Fersht, A. R. (1972) *J. Mol. Biol. 64*, 497–509.

Hekman, C. M., & Loskutoff, D. J. (1985) *J. Biol. Chem. 260*, 11581–11587.

Hekman, C. M., & Loskutoff, D. J. (1988) *Biochemistry 27*, 2911–2918.

Huber, R., & Carrell, R. W. (1989) *Biochemistry 28*, 8951–8966.

Katagiri, K., Okada, K., Hattori, H., & Yano, M. (1988) *Eur. J. Biochem. 176*, 81–87.

Krishnamurti, C., & Alving, B. M. (1992) *Semin. Thromb. Haemostasis 18*, 67–80.

Lambers, J. W., Cammenga, M., Konig, B. W., Mertens, K., Pannekoek, H., & van Mourik, J. A. (1987) *J. Biol. Chem. 262*, 17492–17496.

Lawrence, D. A., & Ginsburg, D. (1994) in *Molecular Biology of Thrombosis and Hemostasis* (Roberts, H. R., & High, K. A., Eds.) Marcel Dekker, Inc., New York (in press).

Lawrence, D. A., Strandberg, L., Grundström, T., & Ny, T. (1989) *Eur. J. Biochem. 186*, 523–533.

Lawrence, D. A., Strandberg, L., Ericson, J., & Ny, T. (1990) *J. Biol. Chem. 265*, 20293–20301.

Levin, E. G., & Santell, L. (1987) *Blood 70*, 1090–1098.

Lindahl, T. L., Sigurdardóttir, O., & Wiman, B. (1989) *Thromb. Haemostasis 62*, 748–751.

Madison, E. L., Goldsmith, E. J., Gerard, R. D., Gething, M. H., & Sambrook, J. F. (1989) *Nature 339*, 721–724.

Madison, E. L., Goldsmith, E. J., Gerard, R. D., Gething, M. H., Sambrook, J. F., & Bassel-Duby, R. S. (1990a) *Proc. Natl. Acad. Sci. U.S.A. 87*, 3530–3533.

Madison, E. L., Goldsmith, E. J., Gething, M.-J. H., Sambrook, J. F., & Gerard, R. D. (1990b) *J. Biol. Chem. 265*, 21423–21426.

Mimuro, J., & Loskutoff, D. J. (1989) *J. Biol. Chem. 264*, 5058–5063.

Moscatelli, D., & Rifkin, D. B. (1988) *Biochim. Biophys. Acta 948*, 67–85.

Mottonen, J., Strand, A., Symersky, J., Sweet, R. M., Danley, D. E., Geoghegan, K. F., Gerard, R. D., & Goldsmith, E. J. (1992) *Nature 355*, 270–273.

Munch, M., Heegaard, C., Jensen, P. H., & Andreasen, P. A. (1991) *FEBS Lett. 295*, 102–106.

Naski, M. C., Lawrence, D. A., Mosher, D. F., Podor, T. J., & Ginsburg, D. (1993) *J. Biol. Chem. 268*, 12367–12372.

Ohlsson, M., Peng, X. R., Liu, Y. X., Jia, X. C., Hsueh, A. J., & Ny, T. (1991) *Semin. Thromb. Haemostasis 17*, 286–290.

Pöllänen, J., Stephens, R. W., & Vaheri, A. (1991) *Adv. Cancer Res. 57*, 273–328.

Saksela, O. (1985) *Biochim. Biophys. Acta 823*, 35–65.

Saksela, O., & Rifkin D. B. (1988) *Annu. Rev. Cell Biol. 4*, 93–126.

Sawdey, M. S., & Loskutoff, D. J. (1991) *J. Clin. Invest. 88*, 1346–1353.

Sherman, P. M., Lawrence, D. A., Yang, A. Y., Vandenberg, E. T., Paielli, D., Olson, S. T., Shore, J. D., & Ginsburg, D. (1992) *J. Biol. Chem. 267*, 7588–7595.

Stein, P. E., Leslie, A. G. W., Finch, J. T., Turnell, W. G., McLaughlin, P. J., & Carrell, R. W. (1990) *Nature 347*, 99–102.

Strandberg, L., Lawrence, D. A., Johansson, L. BA., & Ny, T. (1991) *J. Biol. Chem. 266*, 13852–13858.

Studier, F. W., Rosenberg, A. H., Dunn, J. J., & Dubendorff, J. W. (1990) *Methods Enzymol. 185*, 60–89.

van Mourik, J. A., Lawrence, D. A., & Loskutoff, D. J. (1984) *J. Biol. Chem. 259*, 14914–14921.

Vaughan, D. E., Declerck, P. J., Van Houtte, E., De Mol, M., & Collen, D. (1990) *Circ. Res. 67*, 1281–1286.

Wun, T.-C., Palmier, M. O., Siegel, N. R., & Smith, C. E. (1989) *J. Biol. Chem. 264*, 7862–7868.